Structural Engineering and Mechanics, *Vol. 69, No. 5 (2019) 487-497*
DOI: https://doi.org/10.12989/sem.2019.69.5.487

On exact wave propagation analysis of triclinic material using three-dimensional bi-Helmholtz gradient plate model

Behrouz Karami[*1], Maziar Janghorban[1a] and Abdelouahed Tounsi[2b]

[1]*Department of Mechanical Engineering, Marvdasht Branch, Islamic Azad University, Marvdasht, Iran*
[2]*Material and Hydrology Laboratory, University of Sidi Bel Abbes, Faculty of Technology, Civil Engineering Department, Algeria*

(Received October 11, 2018, Revised January 10, 2019, Accepted January 13, 2019)

Abstract. Rapid advances in the engineering applications can bring further areas to provide the opportunity to manipulate anisotropic structures for direct productivity in design of micro/nano-structures. For the first time, magnetic affected wave characteristics of nanosize plates made of anisotropic material is investigated via the three-dimensional bi-Helmholtz nonlocal strain gradient theory. Three small scale parameters are used to predict the size-dependent behavior of the nanoplates more accurately. After owing governing equations of wave motion, an analytical approach based harmonic series is utilized to fine the wave frequency as well as phase velocity. It is observed that the small scale parameters, magnetic field and wave number have considerable influence on the wave characteristics of anisotropic nanoplates. Due to the lack of any study on the mechanics of three-dimensional bi-Helmholtz gradient plates made of anisotropic materials, it is hoped that the present exact model may be used as a benchmark for future works of such nanostructures.

Keywords: wave propagation; anisotropic materials; three dimensional elasticity theory; magnetic field

1. Introduction

In the current century, due to the rapid development of various industries, the correct and accurate analysis of the various devices is felt more and more. An accurate analysis needs a correct model. Therefore, in the past decades, several theories have been used to model the beam, plate and shell-type structures (Karami *et al.* 2018b, Karami *et al.* 2018f, Shahsavari *et al.* 2018b, Karami *et al.* 2018e, Karami *et al.* 2019a, Li *et al.* 2018, Aguiar *et al.* 2018, Mehar and Panda 2018a, Mehar and Panda 2018b, Katariya and Panda 2018, Mouli *et al.* 2018, Trofimov *et al.* 2018, Mehrabian 2018, Ghayesh 2018b, Ghayesh 2018c). Some of these theories took into account the effect of thickness and predicted more accurately behavior of different structures. For example, three-dimensional (3D) elasticity theory and quasi-3D theories (Karami *et al.* 2017, Shahsavari *et al.* 2018a, Shahsavari *et al.* 2018e). Also, some other theories require a shear modification factor to predict accurate results, but others do not want to (Karami *et al.* 2018a, Karami *et al.* 2018c, Karami *et al.* 2018g, Karami *et al.* 2018h).

In the current study, according to offer more accurate results, three-dimensional elasticity theory is used. This theory is used as a comprehensive theory and due to the opinion of some researchers, is considered as the most accurate and as a theory without any approximation. This theory also has an accurate prediction of the mechanical behavior of different structures considering the thickness effect (ε_z=0). Some of the researchers have been widely used this theory in their articles. To study the vibrational behavior of simply-supported thick plates a 3D elasticity theory using the direct methods were presented by (Srinivas *et al.* 1970). (Malekzadeh 2009) investigated the dynamics of FG plates with simply-supported boundary conditions with the framework of 3D theory of elasticity. To solve the governing equations, a numerical approach was proposed on the basis of differential quadrature method (DQM). (Alibeigloo and Liew 2014) developed an exact solution to study the 3D vibrations of sandwich cylindrical panels including FG core. A 3D model is adopted to investigate the bending and vibrations of the laminated plates by (Malekzadeh and Heydarpour 2015) via a semi-analytical approach.

Many applications of nanostructured materials cannot be concealed due to their crystalline layout and their properties. This range of applications is so extensive that researchers have been driven to investigate their behavior. Accordingly, non-classical continuum theories have been presented to predict the size-dependent behavior of nanostructure systems (i.e., nonlocal elasticity theory (Eringen and Edelen 1972, Boumia *et al.* 2014, Sahmani *et al.* 2015, Besseghier *et al.* 2011, Khaniki 2018, Barretta *et al.* 2018, Khetir *et al.* 2017, Bellifa *et al.* 2017, Kaghazian *et al.* 2017, Karami *et al.* 2019b, Karami *et al.* 2018l, Shahsavari *et al.* 2017, Xu *et al.* 2017, Mehar *et al.* 2018, Bounouara *et al.* 2016, Shahsavari and Janghorban 2017,

*Corresponding author, Ph.D. Student
E-mail: behrouz.karami@miau.ac.ir
[a]Ph.D.
E-mail: maziar.janghorban@miau.ac.ir
[b]Professor
E-mail: tou_abdel@yahoo.com

http://www.techno-press.com/journals/sem&subpage=7 ISSN: 1225-4568 (Print), 1598-6217 (Online)

Besseghier *et al.* 2017), strain gradient theory (Nami and Janghorban 2014b, Karami and Janghorban 2016), modified couple stress theory (Ehyaei and Akbarizadeh 2017, Kocaturk and Akbas 2013, Brach *et al.* 2017, Ghayesh 2018a, Ghayesh and Farokhi 2015, Gholipour *et al.* 2015) and nonlocal strain gradient theory (Li *et al.* 2016, Mehralian *et al.* 2017, Ebrahimi and Barati 2018, Barati 2017b, Zhu and Li 2017, Sahmani and Aghdam 2017b, Ebrahimi and Dabbagh 2018, She *et al.* 2017, She *et al.* 2018d, Shafiei and She 2018, Faleh *et al.* 2018), etc.).

It was previously reported by researchers that the softening/hardening-stiffness mechanisms of nanostructure systems are, respectively, captured via nonlocality and the strain gradient size-dependency. (Lim *et al.* 2015) suggested a size dependent model(so called nonlocal strain gradient theory) in which three small scale parameters predict the size-dependent behavior (two nonlocal parameters and one strain gradient parameter). Based on this theory, several studies have been done so far (Karami *et al.* 2018i, She *et al.* 2018a, Karami *et al.* 2018j, Shahsavari *et al.* 2018c, She *et al.* 2018b, Shahsavari *et al.* 2018d, She *et al.* 2018c, She *et al.* 2019, Barati 2017a, Barati 2018, Shahverdi and Barati 2017). (Nami and Janghorban 2014a) reported the forced resonant vibrations of FG Kirchhoff plates in micro/-nano dimension for the first time. To considering the small-scale effects of nanostructure systems nonlocal and strain gradient theories were used separately. The authors were proved in which these theories, different mechanisms of size-dependency observed. Via the nonlocal strain gradient model of elasticity buckling force of Euler-Bernoulli nanosize beam in nonlinear form were studied by (Li and Hu 2015). In addition, with the same authors size-dependent wave characteristics of fluid-conveying carbon nanotubes via mentioned theory were analyzed (Li and Hu 2016). Wave propagation analysis of single-layer graphene sheets (SLGSs) were investigated by (Karami *et al.* 2018k) based on nonlocal strain gradient theory in conjunction with second order shear deformation plate theory. (Mohammadi *et al.* 2018) presented the dynamics of FG nanoshell for different boundary conditions (i.e., for simply supported and clamped-clamped). The influence of nonlocality and strain gradient size-dependency were obtained with nonlocal strain gradient theory. (Zeighampour *et al.* 2018) proposed a size-dependent model to study the wave propagation of viscoelastic thin cylindrical nanoshell resting on a visco-Pasternak foundation using nonlocal strain gradient theory. (Mehralian and Beni 2018) studied the vibration response of size-dependent bimorph functionally graded piezoelectric cylindrical shell via nonlocal strain gradient theory. (Sahmani and Aghdam 2017a) employed nonlocal strain gradient elasticity theory to study nonlinear vibration of pre-buckled and post-buckled multilayer functionally graded graphene platelet-reinforced composite nanobeams. They also (Sahmani and Aghdam 2018) presented size-dependent post-buckling and associated vibrational response of lipid supramolecular protein micro/nano-tubules based upon nonlocal strain gradient theory.

It is obvious that size-dependent mechanical analysis of isotropic and non-isotropic materials based on the various two-dimensional models are widely used, however, there are few articles that investigate size-dependent mechanical analysis of such structures based on the three-dimensional model. (Karami *et al.* 2018d) presented three-dimensional nonlocal strain gradient spherical model to investigate the radial vibration as well as wave propagation in radial direction of anisotropic nanoparticles. Therefore, there isn't any research on mechanics of anisotropic nanoplates subjected to a biaxial magnetic field based upon three-dimensional bi-Helmholtz gradient model.

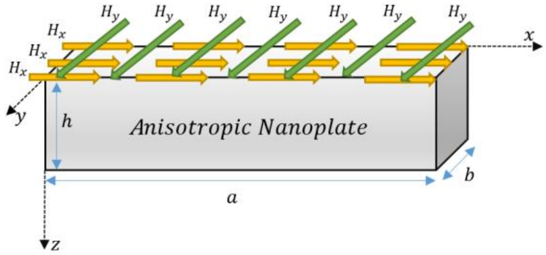

Fig. 1 Geometry of anisotropic nanoplate under be-directional magnetic field effect

In the current work, magnetic affected wave propagation of nanosize plates made of anisotropic materials is presented using three-dimensional bi-Helmholtz gradient theory. Afterward, a parametric numerical sturdy is presented to study the effects of different parameters such as small scale parameters, magnetic potential and wave number.

2. Lorentz force induced by the biaxial magnetic field

Consider a magnetically sensitive rectangular nanoplate made of anisotropic materials with the length of a, width of b and thickness of h placed in biaxial magnetic field $\mathbf{H}$ (H_x, H_y, 0) as shown in Fig. 1. A Cartesian coordinates system (x, y, z) is employed while x and y- coordinates are considered at the bottom plane of nanoplate. Thus, the displacement filed in the Cartesian coordinates can be written as

$$\begin{gathered} u = u\left(x, y, z, t\right), v = v\left(x, y, z, t\right) \\ w = w\left(x, y, z, t\right) \end{gathered} \tag{1}$$

herein u, v, and w are, respectively, components of the displacement vector $\mathbf{U}$, along the x, y and z-axes.

By ignoring the displacement electric current, the Maxwell's equations of the magnetic field can be shown as (Murmu *et al.* 2013)

$$\begin{gathered} \mathbf{J} = \nabla \times \mathbf{h},\ \nabla \times \mathbf{e} = -\eta \frac{\partial \mathbf{h}}{\partial \mathrm{t}},\ \nabla \cdot \mathbf{h} = 0, \\ \mathbf{e} = -\eta \left(\frac{\partial \mathbf{U}}{\partial \mathrm{t}} \times \mathbf{H} \right), \mathbf{h} = \nabla \times \left(\mathbf{U} \times \mathbf{H} \right) \end{gathered} \tag{2}$$

in which $\mathbf{J}$ is the electric current density vector, $\mathbf{h}$ is the perturbation of magnetic field vector, $\mathbf{U}$ (u, v, w) is the plate displacement vector, and η is the magnetic permeability; ∇ is defined as $\nabla = \partial/\partial x\ \mathbf{i} + \partial/\partial y\ \mathbf{j} + \partial/\partial z\ \mathbf{k}$, and $\mathbf{i}$, $\mathbf{j}$, and $\mathbf{k}$

denote the unit vectors in directions x, y, z.

In the present study, biaxial magnetic field on the anisotropic nanoplate in the x- and y-direction is assumed. Distributing the magnetic field vector can be represented as,

$$\mathbf{h}=\nabla\times(\mathbf{U}\times\mathbf{H})=\left\{-H_x(\frac{\partial v}{\partial y}+\frac{\partial w}{\partial z})+H_y\frac{\partial u}{\partial y}\right\}\mathbf{i}+\left\{H_x\frac{\partial v}{\partial x}-H_y(\frac{\partial u}{\partial x}+\frac{\partial w}{\partial z})\right\}\mathbf{j}+\left\{H_x\frac{\partial w}{\partial x}+H_y\frac{\partial w}{\partial y}\right\}\mathbf{k} \tag{3}$$

By substituting Eq. (3) into the first expressions of Eq. (2), we have

$$\begin{aligned}\mathbf{J}=\nabla\times\mathbf{h}=\\ &\left\{H_x(-\frac{\partial^2 v}{\partial x\partial z}+\frac{\partial^2 w}{\partial x\partial y})+H_y(\frac{\partial^2 u}{\partial x\partial z}+\frac{\partial^2 w}{\partial y^2}+\frac{\partial^2 w}{\partial z^2})\right\}\mathbf{i}\\ &+\left\{-H_x(\frac{\partial^2 v}{\partial y\partial z}+\frac{\partial^2 w}{\partial x^2}+\frac{\partial^2 w}{\partial z^2})+H_y(\frac{\partial^2 u}{\partial y\partial z}-\frac{\partial^2 w}{\partial x\partial y})\right\}\mathbf{j}\\ &+\left\{H_x(\frac{\partial^2 v}{\partial x^2}+\frac{\partial^2 v}{\partial y^2}+\frac{\partial^2 w}{\partial y\partial z})-H_y(\frac{\partial^2 u}{\partial x^2}+\frac{\partial^2 u}{\partial y^2}+\frac{\partial^2 w}{\partial x\partial z})\right\}\mathbf{k}\end{aligned} \tag{4}$$

Furthermore, substituting Eq. (4) into relations for the Lorentz force induced by the biaxial magnetic field yields to

$$\begin{aligned}\mathbf{F}&=f_x\mathbf{i}+f_y\mathbf{j}+f_z\mathbf{k}=\eta(\mathbf{J}\times\mathbf{H})\\ &=\eta\left[\left\{-H_xH_y(\frac{\partial^2 v}{\partial x^2}+\frac{\partial^2 v}{\partial y^2}+\frac{\partial^2 w}{\partial y\partial z})+H_y^2(\frac{\partial^2 u}{\partial x^2}+\frac{\partial^2 u}{\partial y^2}+\frac{\partial^2 w}{\partial x\partial z})\right\}\mathbf{i}\right.\\ &+\left\{H_x^2(\frac{\partial^2 v}{\partial x^2}+\frac{\partial^2 v}{\partial y^2}+\frac{\partial^2 w}{\partial y\partial z})-H_xH_y(\frac{\partial^2 u}{\partial x^2}+\frac{\partial^2 u}{\partial y^2}+\frac{\partial^2 w}{\partial x\partial z})\right\}\mathbf{j}\\ &+\left\{H_x^2(\frac{\partial^2 v}{\partial y\partial z}+\frac{\partial^2 w}{\partial x^2}+\frac{\partial^2 w}{\partial z^2})-H_xH_y(\frac{\partial^2 u}{\partial y\partial z}+\frac{\partial^2 v}{\partial x\partial z}-2\frac{\partial^2 w}{\partial x\partial y})\right.\\ &\left.\left.+H_y^2(\frac{\partial^2 u}{\partial x\partial z}+\frac{\partial^2 w}{\partial y^2}+\frac{\partial^2 w}{\partial z^2})\right\}\mathbf{k}\right]\end{aligned} \tag{5}$$

in which f_x, f_y, f_z denote the Lorentz force along the x, y and z- directions, respectively. In present paper, it is assumed that the Lorentz force exists only in the z-direction. So, we have

$$\begin{aligned}f_z=\eta&\left\{H_x^2(\frac{\partial^2 v}{\partial y\partial z}+\frac{\partial^2 w}{\partial x^2}+\frac{\partial^2 w}{\partial z^2})-H_xH_y(\frac{\partial^2 u}{\partial y\partial z}+\frac{\partial^2 v}{\partial x\partial z}-2\frac{\partial^2 w}{\partial x\partial y})\right.\\ &\left.+H_y^2(\frac{\partial^2 u}{\partial x\partial z}+\frac{\partial^2 w}{\partial y^2}+\frac{\partial^2 w}{\partial z^2})\right\}\end{aligned} \tag{6}$$

3. problem formulation

3.1 Bi-Helmholtz gradient theory

To consider the small scale effects following non-classical stress-strain relation proposed by (Lim *et al.* 2015) is introduced

$$\sigma_{ij}=\sigma_{ij}^{(0)}-\nabla\sigma_{ij}^{(1)} \tag{7}$$

in which $\sigma_{ij}^{(0)}$ and $\sigma_{ij}^{(1)}$ are corresponding, respectively, to strain ε_{ij} and strain gradient $\nabla\varepsilon_{ij}$,

$$\sigma_{ij}^{(0)}=\int_V C_{ijkl}\alpha_0(x,x',e_0a)\varepsilon'_{kl}(x')dx' \tag{8}$$

$$\sigma_{ij}^{(0)}=\int_V C_{ijkl}\alpha_0(x,x',e_0a)\varepsilon'_{kl}(x')dx' \tag{9}$$

where Q_{ijkl} are the elastic coefficients; l is strain gradient parameter; e_0a and e_1a are lower and higher nonlocal parameters, respectively. $\alpha_0(x,x',e_0a)$ and $\alpha_1(x,x',e_1a)$ denote the classical and gradient stress tensors of nonlocal functions (Eringen 1983). The linear nonlocal differential operator $\mathrm{L}l_i$, which is going to be applied to the both sides of Eq. (7), is defined as

$$\mathrm{L}l_i=1-(e_ia)^2\nabla^2 \qquad \text{for } i=0,1 \tag{10}$$

where ∇^2 is the Laplacian operator. It is important to note that unlike some other studies, in our continuum theory we include the thickness effect (z- direction) on the mechanism of small-scale effects. So, Laplacian operator for 3D problems can be defined as

$$\nabla^2=\partial^2/\partial x^2+\partial^2/\partial y^2+\partial^2/\partial z^2 \tag{11}$$

By applying Eq. (10) into Eq. (7), the consequent differential constitutive equation for nonlocal gradient materials can be expressed as (Lim *et al.* 2015)

$$\begin{aligned}&\left[1-(e_1a)^2\nabla^2\right]\left[1-(e_0a)^2\nabla^2\right]\sigma_{ij}=C_{ijkl}\left[1-(e_1a)^2\nabla^2\right]\varepsilon_{kl}\\ &-C_{ijkl}l^2\left[1-(e_0a)^2\nabla^2\right]\nabla^2\varepsilon_{kl}\end{aligned} \tag{12}$$

Let $\mu_0=e_0a$, $\mu_1=e_0a$. consequently, the general constitutive equation of bi-Helmholtz gradient theory is defined as (Lim *et al.* 2015)

$$(1-\mu_1^2\nabla^2)(1-\mu_0^2\nabla^2)\sigma_{ij}=C_{ijkl}\left[(1-\mu_1^2\nabla^2)\varepsilon_{kl}-l^2(1-\mu_0^2\nabla^2)\nabla^2\varepsilon_{kl}\right] \tag{13}$$

The equivalent form of Eq. (13) is presented as

$$\mathrm{L}_\mu\sigma_{ij}=C_{ijkl}\mathrm{L}_l\varepsilon_{kl} \tag{14}$$

where the linear operators are defined as

$$\mathrm{L}_\mu=(1-\mu_1^2\nabla^2)(1-\mu_0^2\nabla^2),\mathrm{L}_l=(1-\mu_1^2\nabla^2)-l^2(1-\mu_0^2\nabla^2)\nabla^2 \tag{15}$$

3.2 Equations of motion

The equations of motion of the plate are extracted with regard to Hamilton's principle given as

$$\sigma_{ij}=\sigma_{ij}^{(0)}-\nabla\sigma_{ij}^{(1)} \tag{16}$$

in which K and U are virtual kinematic and strain energies, and W is the virtual work done by the external forces. The variation of the virtual kinematic energy of present plate model is described as

$$\delta K=\int_0^h\int_0^b\int_0^a\rho\left(\frac{\partial u}{\partial t}\delta(\frac{\partial u}{\partial t})+\frac{\partial v}{\partial t}\delta(\frac{\partial v}{\partial t})+\frac{\partial w}{\partial t}\delta(\frac{\partial w}{\partial t})\right)dxdydz \tag{17}$$

in which ρ is mass density.

The variation of virtual work done by external forces and couples expressed is as

$$\delta W = \int_v \left(f_x \delta u + f_y \delta v + f_z \delta w \right) dV \tag{18}$$

The variation of virtual strain energy can be written as

$$\delta U = \int_0^h \int_0^b \int_0^a \begin{pmatrix} \sigma_{xx}\delta\varepsilon_{xx} + \sigma_{yy}\delta\varepsilon_{yy} + \sigma_{zz}\delta\varepsilon_{zz} \\ +2\sigma_{xy}\delta\varepsilon_{xy} + 2\sigma_{xz}\delta\varepsilon_{xz} + 2\sigma_{yz}\delta\varepsilon_{yz} \end{pmatrix} dxdydz$$

$$= \int_0^h \int_0^b \int_0^a \left(\sigma_{xx}\frac{\partial \delta u}{\partial x} + \sigma_{yy}\frac{\partial \delta v}{\partial x} + \sigma_{xx}\frac{\partial \delta w}{\partial x} + \sigma_{xy}\left(\frac{\partial \delta u}{\partial y} + \frac{\partial \delta v}{\partial x}\right) \right. \tag{19}$$

$$\left. +\sigma_{xz}\left(\frac{\partial \delta u}{\partial z} + \frac{w}{\partial b}\right) + \sigma_{yz}\left(\frac{\partial \delta v}{z} + \frac{\partial \delta w}{\partial y}\right) \right) dxdydz$$

By inserting δK, δW and δU from Eqs. (17)-(19) in Eq. (16) and using the integration-by-parts and setting the coefficients ∂u, ∂v and ∂w to zero, three-dimensional equations of motion can be derived as

$$\delta u: \frac{\partial \sigma_{xx}}{\partial x} + \frac{\partial \sigma_{xy}}{\partial y} + \frac{\partial \sigma_{xz}}{\partial z} + f_x = \rho \frac{\partial^2 u}{\partial t^2} \tag{20}$$

$$\delta v: \frac{\partial \sigma_{xy}}{\partial x} + \frac{\partial \sigma_{yy}}{\partial y} + \frac{\partial \sigma_{yz}}{\partial z} + f_y = \rho \frac{\partial^2 v}{\partial t^2} \tag{21}$$

$$\delta w: \frac{\partial \sigma_{xz}}{\partial x} + \frac{\partial \sigma_{yz}}{\partial y} + \frac{\partial \sigma_{zz}}{\partial z} + f_z = \rho \frac{\partial^2 w}{\partial t^2} \tag{22}$$

herein f_i (i=x, y, z) denote the body forces (see in Eq. (6)). The equations of motion (20)-(22) are in terms of stress components σ. With regard to three-dimensional linear elasticity and bi-Helmholtz gradient theories,

$$\mathrm{L}_\mu \begin{Bmatrix} \sigma_{xx} \\ \sigma_{yy} \\ \sigma_{zz} \\ \tau_{yz} \\ \tau_{xz} \\ \tau_{xy} \end{Bmatrix} = \begin{bmatrix} C_{11} & C_{12} & C_{13} & C_{14} & C_{15} & C_{16} \\ C_{21} & C_{22} & C_{23} & C_{24} & C_{25} & C_{26} \\ C_{31} & C_{32} & C_{33} & C_{34} & C_{35} & C_{36} \\ C_{41} & C_{42} & C_{43} & C_{44} & C_{45} & C_{46} \\ C_{51} & C_{52} & C_{53} & C_{54} & C_{55} & C_{56} \\ C_{61} & C_{62} & C_{63} & C_{64} & C_{65} & C_{66} \end{bmatrix} \mathrm{L}_l \begin{Bmatrix} \varepsilon_{xx} \\ \varepsilon_{yy} \\ \varepsilon_{zz} \\ \gamma_{yz} \\ \gamma_{xz} \\ \gamma_{xy} \end{Bmatrix} \tag{23}$$

By substituting Eq. (23) into Eqs. (20)-(22), the equations of motion are obtained in terms of displacements as

$$\begin{aligned}
&\mathrm{L}_l\left(\frac{\partial C_{11}}{\partial x}\frac{\partial u}{\partial x} + C_{11}\frac{\partial^2 u}{\partial x^2} + \frac{\partial C_{12}}{\partial x}\frac{\partial v}{\partial y} + C_{12}\frac{\partial^2 v}{\partial x \partial y} + \frac{\partial C_{13}}{\partial x}\frac{\partial w}{\partial z} + C_{13}\frac{\partial^2 w}{\partial x \partial z} + \frac{\partial C_{14}}{\partial x}\left(\frac{\partial v}{\partial z} + \frac{\partial w}{\partial y}\right)\right) \\
&+\mathrm{L}_l\left(C_{14}\left(\frac{\partial^2 v}{\partial x \partial z} + \frac{\partial^2 w}{\partial x \partial y}\right) + \frac{\partial C_{15}}{\partial x}\left(\frac{\partial w}{\partial x} + \frac{\partial u}{\partial z}\right) + C_{15}\left(\frac{\partial^2 w}{\partial x^2} + \frac{\partial^2 u}{\partial x \partial z}\right) + \frac{\partial C_{16}}{\partial x}\left(\frac{\partial u}{\partial y} + \frac{\partial v}{\partial x}\right)\right) \\
&+\mathrm{L}_l\left(C_{16}\left(\frac{\partial^2 u}{\partial x \partial y} + \frac{\partial^2 v}{\partial x^2}\right) + \frac{\partial C_{61}}{\partial y}\frac{\partial u}{\partial x} + C_{61}\frac{\partial^2 u}{\partial x \partial y} + \frac{\partial C_{62}}{\partial y}\frac{\partial v}{\partial y} + C_{62}\frac{\partial^2 v}{\partial y^2} + \frac{\partial C_{63}}{\partial y}\frac{\partial w}{\partial z} + C_{63}\frac{\partial^2 w}{\partial y \partial z}\right) \\
&+\mathrm{L}_l\left(\frac{\partial C_{64}}{\partial y}\left(\frac{\partial v}{\partial z} + \frac{\partial w}{\partial y}\right) + C_{64} + \left(\frac{\partial^2 v}{\partial y \partial z} + \frac{\partial^2 w}{\partial y^2}\right) + \frac{\partial C_{65}}{\partial y}\left(\frac{\partial w}{\partial x} + \frac{\partial u}{\partial z}\right) + C_{65}\left(\frac{\partial^2 w}{\partial x \partial y} + \frac{\partial^2 u}{\partial y \partial z}\right)\right) \\
&+\mathrm{L}_l\left(\frac{\partial C_{66}}{\partial y}\left(\frac{\partial u}{\partial y} + \frac{\partial v}{\partial x}\right) + C_{66}\left(\frac{\partial^2 u}{\partial y^2} + \frac{\partial^2 v}{\partial x \partial y}\right) + \frac{\partial C_{51}}{\partial z}\frac{\partial u}{\partial x} + C_{51}\frac{\partial^2 u}{\partial x \partial z} + \frac{\partial C_{52}}{\partial z}\frac{\partial v}{\partial y} + C_{52}\frac{\partial^2 v}{\partial y \partial z}\right) \\
&+\mathrm{L}_l\left(\frac{\partial C_{53}}{\partial z}\frac{\partial w}{\partial z} + C_{53}\frac{\partial^2 w}{\partial z^2} + \frac{\partial C_{54}}{\partial z}\left(\frac{\partial v}{\partial z} + \frac{\partial w}{\partial y}\right) + C_{54}\left(\frac{\partial^2 v}{\partial z^2} + \frac{\partial^2 w}{\partial z \partial y}\right) + \frac{\partial C_{55}}{\partial z}\left(\frac{\partial w}{\partial x} + \frac{\partial u}{\partial z}\right)\right) \\
&+\mathrm{L}_l\left(C_{55}\left(\frac{\partial^2 w}{\partial x \partial z} + \frac{\partial^2 u}{\partial z^2}\right) + \frac{\partial C_{56}}{\partial z}\left(\frac{\partial u}{\partial y} + \frac{\partial v}{\partial x}\right) + C_{56}\left(\frac{\partial^2 u}{\partial y \partial z} + \frac{\partial^2 v}{\partial x \partial z}\right)\right) + \mathrm{L}_\mu\left(f_x - \rho\frac{\partial^2 u}{\partial t^2}\right) = 0
\end{aligned} \tag{24}$$

$$\begin{aligned}
&\mathrm{L}_l\left(\frac{\partial C_{61}}{\partial x}\frac{\partial u}{\partial x} + C_{61}\frac{\partial^2 u}{\partial x^2} + \frac{\partial C_{62}}{\partial x}\frac{\partial v}{\partial y} + C_{62}\frac{\partial^2 v}{\partial x \partial y} + \frac{\partial C_{63}}{\partial x}\frac{\partial w}{\partial z} + C_{63}\frac{\partial^2 w}{\partial x \partial z} + \frac{\partial C_{64}}{\partial x}\left(\frac{\partial v}{\partial z} + \frac{\partial w}{\partial y}\right)\right) \\
&+\mathrm{L}_l\left(C_{64}\left(\frac{\partial^2 v}{\partial x \partial z} + \frac{\partial^2 w}{\partial x \partial y}\right) + \frac{\partial C_{65}}{\partial x}\left(\frac{\partial w}{\partial x} + \frac{\partial u}{\partial z}\right) + C_{65}\left(\frac{\partial^2 w}{\partial x^2} + \frac{\partial^2 u}{\partial x \partial z}\right) + \frac{\partial C_{66}}{\partial x}\left(\frac{\partial u}{\partial y} + \frac{\partial v}{\partial x}\right)\right) \\
&+\mathrm{L}_l\left(C_{66}\left(\frac{\partial^2 u}{\partial x \partial y} + \frac{\partial^2 v}{\partial x^2}\right) + \frac{\partial C_{21}}{\partial y}\frac{\partial u}{\partial x} + C_{21}\frac{\partial^2 u}{\partial x \partial y} + \frac{\partial C_{22}}{\partial y}\frac{\partial v}{\partial y} + C_{22}\frac{\partial^2 v}{\partial y^2} + \frac{\partial C_{23}}{\partial y}\frac{\partial w}{\partial z} + C_{23}\frac{\partial^2 w}{\partial y \partial z}\right) \\
&+\mathrm{L}_l\left(\frac{\partial C_{24}}{\partial y}\left(\frac{\partial v}{\partial z} + \frac{\partial w}{\partial y}\right) + C_{24} + \left(\frac{\partial^2 v}{\partial y \partial z} + \frac{\partial^2 w}{\partial y^2}\right) + \frac{\partial C_{25}}{\partial y}\left(\frac{\partial w}{\partial x} + \frac{\partial u}{\partial z}\right) + C_{25}\left(\frac{\partial^2 w}{\partial x \partial y} + \frac{\partial^2 u}{\partial y \partial z}\right)\right) \\
&+\mathrm{L}_l\left(\frac{\partial C_{26}}{\partial y}\left(\frac{\partial u}{\partial y} + \frac{\partial v}{\partial x}\right) + C_{26}\left(\frac{\partial^2 u}{\partial y^2} + \frac{\partial^2 v}{\partial x \partial y}\right) + \frac{\partial C_{41}}{\partial z}\frac{\partial u}{\partial x} + C_{41}\frac{\partial^2 u}{\partial x \partial z} + \frac{\partial C_{42}}{\partial z}\frac{\partial v}{\partial y} + C_{42}\frac{\partial^2 v}{\partial y \partial z}\right) \\
&+\mathrm{L}_l\left(\frac{\partial C_{43}}{\partial z}\frac{\partial w}{\partial z} + C_{43}\frac{\partial^2 w}{\partial z^2} + \frac{\partial C_{44}}{\partial z}\left(\frac{\partial v}{\partial z} + \frac{\partial w}{\partial y}\right) + C_{44}\left(\frac{\partial^2 v}{\partial z^2} + \frac{\partial^2 w}{\partial z \partial y}\right) + \frac{\partial C_{45}}{\partial z}\left(\frac{\partial w}{\partial x} + \frac{\partial u}{\partial z}\right)\right) \\
&+\mathrm{L}_l\left(C_{45}\left(\frac{\partial^2 w}{\partial x \partial z} + \frac{\partial^2 u}{\partial z^2}\right) + \frac{\partial C_{46}}{\partial z}\left(\frac{\partial u}{\partial y} + \frac{\partial v}{\partial x}\right) + C_{46}\left(\frac{\partial^2 u}{\partial y \partial z} + \frac{\partial^2 v}{\partial x \partial z}\right)\right) + \mathrm{L}_\mu\left(f_y - \rho\frac{\partial^2 v}{\partial t^2}\right) = 0
\end{aligned} \tag{25}$$

$$\begin{aligned}
&\mathrm{L}_l\left(\frac{\partial C_{51}}{\partial x}\frac{\partial u}{\partial x} + C_{51}\frac{\partial^2 u}{\partial x^2} + \frac{\partial C_{52}}{\partial x}\frac{\partial v}{\partial y} + C_{52}\frac{\partial^2 v}{\partial x \partial y} + \frac{\partial C_{53}}{\partial x}\frac{\partial w}{\partial z} + C_{53}\frac{\partial^2 w}{\partial x \partial z} + \frac{\partial C_{54}}{\partial x}\left(\frac{\partial v}{\partial z} + \frac{\partial w}{\partial y}\right)\right) \\
&+\mathrm{L}_l\left(C_{54}\left(\frac{\partial^2 v}{\partial x \partial z} + \frac{\partial^2 w}{\partial x \partial y}\right) + \frac{\partial C_{55}}{\partial x}\left(\frac{\partial w}{\partial x} + \frac{\partial u}{\partial z}\right) + C_{55}\left(\frac{\partial^2 w}{\partial x^2} + \frac{\partial^2 u}{\partial x \partial z}\right) + \frac{\partial C_{56}}{\partial x}\left(\frac{\partial u}{\partial y} + \frac{\partial v}{\partial x}\right)\right) \\
&+\mathrm{L}_l\left(C_{56}\left(\frac{\partial^2 u}{\partial x \partial y} + \frac{\partial^2 v}{\partial x^2}\right) + \frac{\partial C_{41}}{\partial y}\frac{\partial u}{\partial x} + C_{41}\frac{\partial^2 u}{\partial x \partial y} + \frac{\partial C_{42}}{\partial y}\frac{\partial v}{\partial y} + C_{42}\frac{\partial^2 v}{\partial y^2} + \frac{\partial C_{43}}{\partial y}\frac{\partial w}{\partial z} + C_{43}\frac{\partial^2 w}{\partial y \partial z}\right) \\
&+\mathrm{L}_l\left(\frac{\partial C_{44}}{\partial y}\left(\frac{\partial v}{\partial z} + \frac{\partial w}{\partial y}\right) + C_{44} + \left(\frac{\partial^2 v}{\partial y \partial z} + \frac{\partial^2 w}{\partial y^2}\right) + \frac{\partial C_{45}}{\partial y}\left(\frac{\partial w}{\partial x} + \frac{\partial u}{\partial z}\right) + C_{45}\left(\frac{\partial^2 w}{\partial x \partial y} + \frac{\partial^2 u}{\partial y \partial z}\right)\right) \\
&+\mathrm{L}_l\left(\frac{\partial C_{46}}{\partial y}\left(\frac{\partial u}{\partial y} + \frac{\partial v}{\partial x}\right) + C_{46}\left(\frac{\partial^2 u}{\partial y^2} + \frac{\partial^2 v}{\partial x \partial y}\right) + \frac{\partial C_{31}}{\partial z}\frac{\partial u}{\partial x} + C_{31}\frac{\partial^2 u}{\partial x \partial z} + \frac{\partial C_{32}}{\partial z}\frac{\partial v}{\partial y} + C_{32}\frac{\partial^2 v}{\partial y \partial z}\right) \\
&+\mathrm{L}_l\left(\frac{\partial C_{33}}{\partial z}\frac{\partial w}{\partial z} + C_{33}\frac{\partial^2 w}{\partial z^2} + \frac{\partial C_{34}}{\partial z}\left(\frac{\partial v}{\partial z} + \frac{\partial w}{\partial y}\right) + C_{34}\left(\frac{\partial^2 v}{\partial z^2} + \frac{\partial^2 w}{\partial z \partial y}\right) + \frac{\partial C_{35}}{\partial z}\left(\frac{\partial w}{\partial x} + \frac{\partial u}{\partial z}\right)\right) \\
&+\mathrm{L}_l\left(C_{35}\left(\frac{\partial^2 w}{\partial x \partial z} + \frac{\partial^2 u}{\partial z^2}\right) + \frac{\partial C_{36}}{\partial z}\left(\frac{\partial u}{\partial y} + \frac{\partial v}{\partial x}\right) + C_{36}\left(\frac{\partial^2 u}{\partial y \partial z} + \frac{\partial^2 v}{\partial x \partial z}\right)\right) + \mathrm{L}_\mu\left(f_z - \rho\frac{\partial^2 w}{\partial t^2}\right) = 0
\end{aligned} \tag{26}$$

3.3 Anisotropic materials

With regard to the wonderful properties of anisotropic materials which is due to its elastic constants, these materials have been widely used as a special part of different engineering systems. In this paper, one of the most used non-isotropic materials, named Triclinic is selected to examine its mechanical behavior. For triclinic materials, the elastic constants are defied as follow (Batra *et al.* 2004),

$$\begin{bmatrix} 98.84 & 53.92 & 50.78 & -0.10 & 1.05 & 0.03 \\ & 99.19 & 50.87 & -0.18 & 0.55 & 0.03 \\ & & 87.23 & -0.18 & 1.03 & 0.02 \\ & \text{sym.} & & 21.4 & 0.07 & 0.25 \\ & & & & 21.10 & -0.04 \\ & & & & & 22.55 \end{bmatrix} \times \text{GPa} \tag{27}$$

and ρ=7750 kg/m^3.

3.4 Wave propagation analysis

In this subsection, to analyze the wave propagation in anisotropic nanosize plate, displacements along u, v, and w is expressed as follows

$$u(x,y,z,t) = A_1 e^{i(xk_1 + yk_2 + zk_3 - \omega t)} \tag{28}$$

$$v(x,y,z,t) = A_2 e^{i(xk_1 + yk_2 + zk_3 - \omega t)} \tag{29}$$

$$w(x,y,z,t) = A_3 e^{i(xk_1 + yk_2 + zk_3 - \omega t)} \tag{30}$$

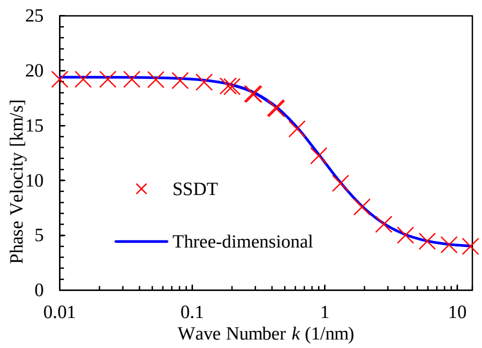

Fig. 2 Comparison of nonlocal strain gradient wave dispersion curves for rectangular nanoplate, (l=0.2 nm, μ=1 nm)

Table 1 First pair of distinct dispersion modes T_1 of wave frequency (THz) in rectangular anisotropic nanoplate

		$H_x=H_y=0$			H_x=1*10^8 A/m, H_y=0 (uniaxial)			$H_x=H_y$=1*10^8 A/m (biaxial)		
		l (nm)								
μ_0 (nm)	μ_1 (nm)	0	1	2	0	1	2	0	1	2
0	0	1.0186	2.0372	3.6726	9.0937	9.1856	9.4711	15.7118	15.753	15.879
	1	1.0186	1.3475	2.0372	4.5928	4.6396	4.7846	7.8766	7.8974	7.9609
	2	1.0186	1.1300	1.4126	2.6268	2.6540	2.7379	4.4041	4.4159	4.4520
1	0	0.5093	1.8363	3.5651	4.5468	4.7356	5.3609	7.8559	7.9396	8.2071
	1	0.5093	1.0186	1.8363	2.2964	2.3923	2.7078	3.9383	3.9804	4.1153
	2	0.5093	0.7063	1.1032	1.3134	1.3689	1.5477	2.2020	2.2260	2.3025
2	0	0.2825	1.7868	3.5398	2.5221	2.8836	4.0440	4.3576	4.5141	5.0771
	1	0.2825	0.9263	1.7868	1.2738	1.4567	2.0358	2.1846	2.2634	2.5466
	2	0.2825	0.5650	1.0186	0.7285	0.8332	1.1521	1.2215	1.2662	1.4260

where A_1, A_2, A_3 are displacement amplitudes; k_1, k_2, and k_3 are wave numbers along x, y, and z-directions.

By substituting Eqs. (29)-(31) into Eqs. (24)-(26) and by solving the problem, the eigenvalue of the frequencies is computed. Besides, by setting k_1=k_2=k_3=k phase velocity is defined as

$$c = \omega / k \tag{31}$$

4. Numerical examples

Using three-dimensional bi-Helmholtz gradient model, no results have been published in the open literature for the mechanics of anisotropic nanoplates. To investigation the three dimensionally mechanics of nanostructures, we considered the thickness effect (z-direction) in our model for considering small-scale effects.

The accuracy of present mathematical model is validate for the phase velocity of nonlocal strain gradient nanoplate with those obtained by (Karami *et al.* 2018k) using second order plate theory SSDT (see in Fig. 2). It is worth noting that, for the nanoplates following materials properties are considered: Young's modulus E=1.06 TPa, density ρ=2250 kg/m^3, and the Poisson's ratio ν=0.25. Good agreement can be seen for two different mathematical models.

Increasingly, these days the better understanding of mechanical behavior of anisotropic structures is felt. So, one of the aims of this study is to provide the exact response of rectangular nanosize plate made of anisotropic materials with respect to small scale parameters for served as a benchmark results for future works. It is worth mentioning that, following numerical examples are calculated for anisotropic materials with properties that reported for Triclinic material (see Eq. (27)). As a benchmark table, wave response of anisotropic nanoplate for three pairs of distinct dispersion modes (T_1, T_2, T_3), for different nonlocal parameters (μ_0 and μ_1) strain gradient length scale parameter (l), and magnetic potential has been tabulated in Tables 1-3. As can be seen, the increment of nonlocal parameters (μ_0 and μ_1) and strain gradient length scale parameter (l), respectively, lead increasing and decreasing the results of anisotropic nanoplate. According to the results presented in this table, we find that higher order nonlocal parameter (μ_1) is inefficient in the absence of a strain gradient parameter (l). The lower-order nonlocal parameter (μ_0) in comparison with higher-order one (μ_1) decreased frequencies of the nanoplate more scientifically at small

Table 2 Second pair of distinct dispersion modes T_2 of wave frequency (THz) in rectangular anisotropic nanoplate

		$H_x=H_y=0$			H_x=1*10^8 A/m, H_y=0 (uniaxial)			$H_x=H_y$=1*10^8 A/m (biaxial)		
		l (nm)								
μ_0 (nm)	μ_1 (nm)	0	1	2	0	1	2	0	1	2
0	0	0.4631	0.9262	1.6698	0.7749	0.9351	1.6862	0.8496	1.6964	3.0431
	1	0.4631	0.6127	0.9262	0.7699	1.0116	1.4986	0.8482	1.1202	1.6851
	2	0.4631	0.5138	0.6422	0.7545	0.8313	1.0175	0.8440	0.9347	1.1624
1	0	0.2316	0.8349	1.6209	0.3875	1.6386	2.4262	0.4248	1.5215	2.8914
	1	0.2316	0.4631	0.8349	0.3849	0.7493	1.2410	0.4241	0.8425	1.4865
	2	0.2316	0.3211	0.5016	0.3772	0.5087	0.7302	0.4220	0.5812	0.8879
2	0	0.1284	0.8123	1.6094	0.2149	1.2421	1.9561	0.2356	1.4572	2.6618
	1	0.1284	0.4211	0.8124	0.2135	0.6393	0.9829	0.2353	0.7540	1.3405
	2	0.1284	0.2569	0.4631	0.2093	0.3818	0.5531	0.2341	0.4574	0.7591

Table 3 Third pair of distinct dispersion modes T_3 of wave frequency (THz) in rectangular anisotropic nanoplate

		$H_x=H_y=0$			H_x=1*10^8 A/m, H_y=0 (uniaxial)			$H_x=H_y$=1*10^8 A/m (biaxial)		
		l (nm)								
μ_0 (nm)	μ_1 (nm)	0	1	2	0	1	2	0	1	2
0	0	0.3425	0.6850	1.2349	0.4675	1.5397	2.7203	0.4664	0.9329	1.6818
	1	0.3425	0.4531	0.6850	0.4675	0.6186	0.9354	0.4664	0.6170	0.9329
	2	0.3425	0.3800	0.4750	0.4676	0.5189	0.6488	0.4665	0.5175	0.6469
1	0	0.1712	0.6174	1.1987	0.2338	0.8431	1.6386	0.2332	0.8409	1.6329
	1	0.1712	0.3425	0.6174	0.2338	0.4677	0.8441	0.2332	0.4665	0.8411
	2	0.1712	0.2375	0.3710	0.2338	0.3244	0.5073	0.2332	0.3234	0.5053
2	0	0.0950	0.6008	1.1902	0.1297	0.8210	1.6360	0.1293	0.8183	1.6222
	1	0.0950	0.3114	0.6008	0.1297	0.4257	0.8260	0.1294	0.4242	0.8188
	2	0.0950	0.1900	0.3425	0.1297	0.2597	0.4713	0.1294	0.2588	0.4668

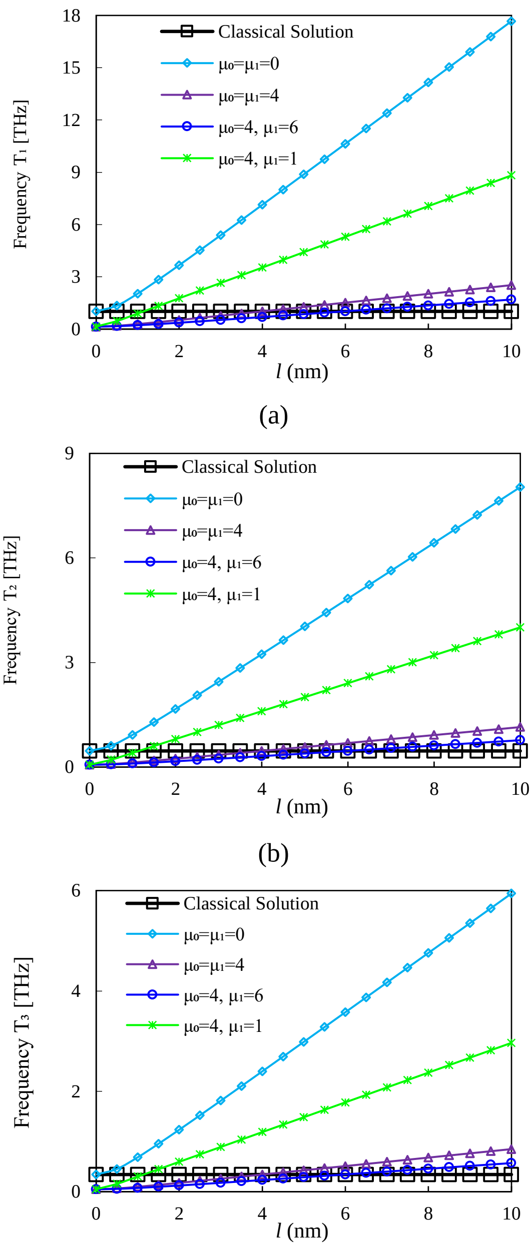

(c)

Fig. 3 Variations of the three pairs of distinct dispersion modes of the rectangular anisotropic nanoplate versus strain gradient length scale parameter and nonlocal parameters

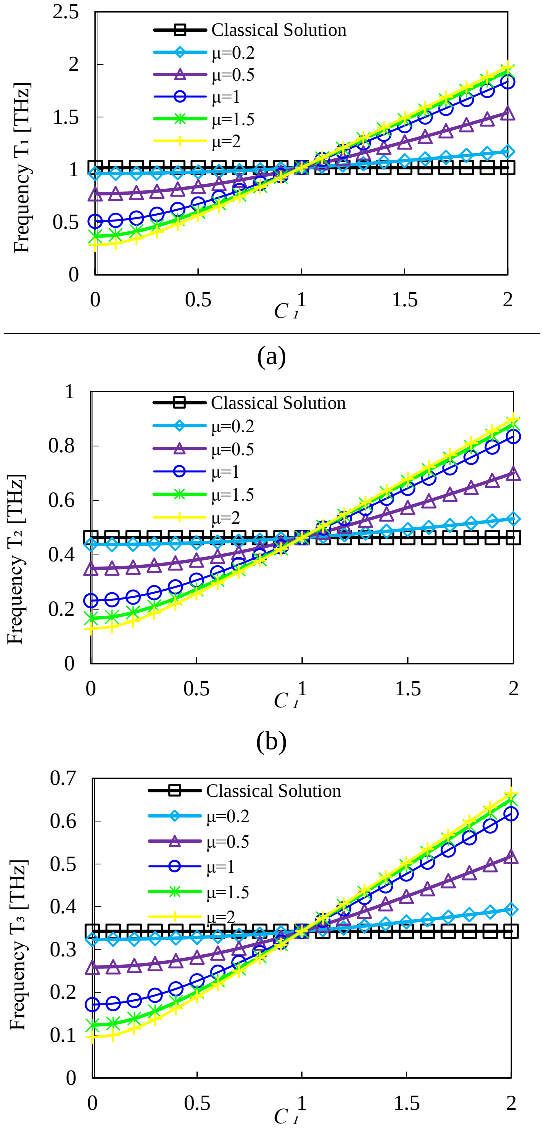

(c)

Fig. 4 The variation of the three pairs of distinct dispersion modes against (C_1) of anisotropic nanoplates (k=1 1/nm)

quantities of the strain gradient parameter (l), while the higher-order nonlocal parameter (μ_1) has more sufficient impact on the frequencies at large amounts of the strain gradient sparaemter (l), compared with lower-order one (μ_0). In order to better understanding of this issue, the three pairs of distinct dispersion modes (T_1, T_2, T_3) of the nanoplate is illustrated in Fig. 3 versus raising the strain gradient parameter (l) and various values of nonlocal parameters (μ_0 and μ_1) when k=1 1/nm.

Next, the impacts of nonlocality and strain gradient size-dependency on wave characteristics of the nanoplates is examined. Fig. 4 plots the three pairs of distinct dispersion modes of wave frequency in anisotropic nanoplates with respect to the scale ratio ($C_1=l/\mu$, $\mu=\mu_0=\mu_1$) for different values of nonlocal parameter (μ). It can be seen that when the nonlocal parameter equals to strain gradient parameter ($l/\mu=1$), the nonlocal strain gradient theory and classical continuum theory predict the same results for wave frequencies for all distinct dispersion modes. However, nonlocal strain gradient theory results are higher than those of classical continuum theory when ($l/\mu>1$), and lower than those of classical continuum theory when ($l/\mu<1$). In other words, strain gradient effect is more important than nonlocal effect when ($l/\mu>1$), resulting in a hardening-type mechanism of the dynamic response and nonlocal effect plays a dominant role when ($l/\mu<1$), leading to a softening-type behavior.

Three pairs of distinct dispersion modes of anisotropic nanoplate due to differences in small-scale parameters is illustrated in Fig. 5. A new scale factor (C_2) has been applied to study the trend of wave frequency in anisotropic

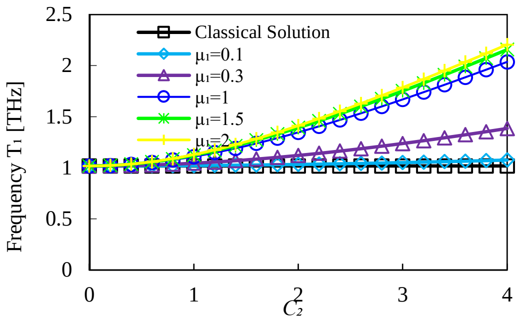

(a)

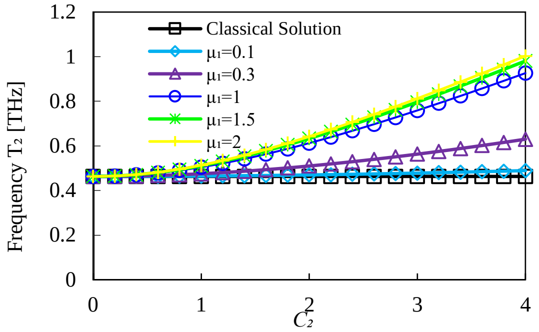

(b)

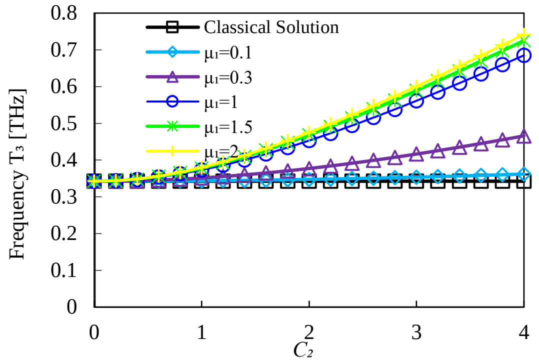

(c)

Fig. 5 The variation of three pairs of distinct dispersion modes of anisotropic nanoplates with respect to scale factor (C_2) and higher-order nonlocal parameter (k=1 1/nm)

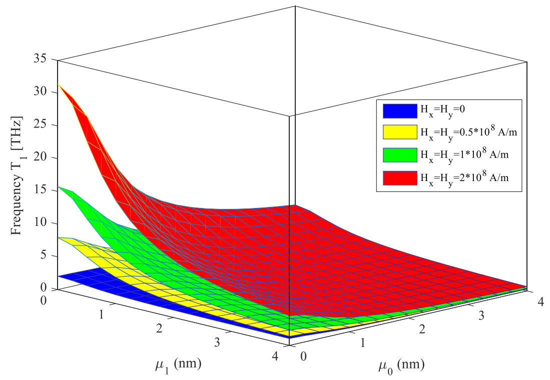

(a)

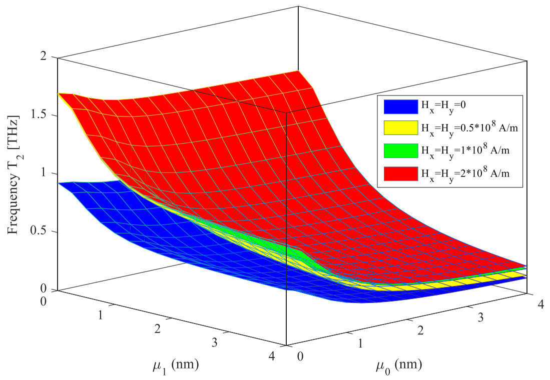

(b)

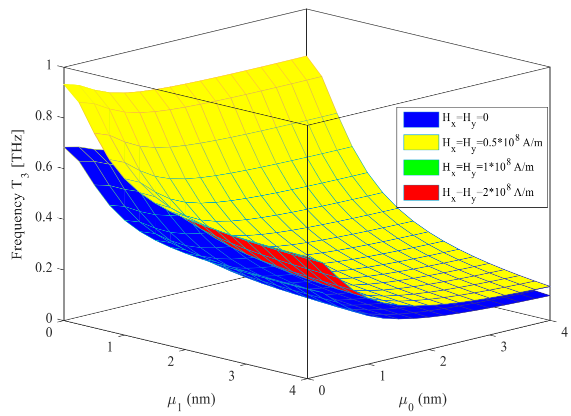

(c)

Fig. 6 The variation of the three pairs of distinct dispersion modes against biaxial magnetic field (k=1 1/nm, l=1 nm)

nanoplate as follows

$$C_2 = l/\mu_1 ,\ \mu_0 = C_2$$

It is obvious that by adopting different values for small-scale parameters, the variations in the responses of rectangular nanoplates will occur. In almost most of cases, the wave frequency rises by raising the scale factor for different values for higher-order nonlocal parameter (μ_1), Similar trend for other pairs of distinct dispersion modes of wave propagation can be seen with respect to different small-scale parameters.

To show the effects of nonlocal stress field and biaxial magnetic field, variation of three pairs of distinct dispersion modes for wave propagation in rectangular anisotropic nanoplates versus the lower and higher order nonlocal parameters is depicted in Fig. 6. The curves are plotted for the wave number k=1 1/nm. From Fig. 6, it is concluded that the wave frequency decrease by increasing the lower and higher nonlocal parameters. Also, the magnetic potential has increasing and decreasing effects in different modes of wave propagation. It is evident that the rate of increasing effect of magnetic field is more when we study the first pairs of distinct dispersion modes of wave propagation. Also, it is obvious that the effect of lower order nonlocal parameter on the wave frequency of the all pairs of distinct dispersion modes increases by increasing the higher order nonlocal parameter. This trend is completely similar for the wave frequency of the three pairs

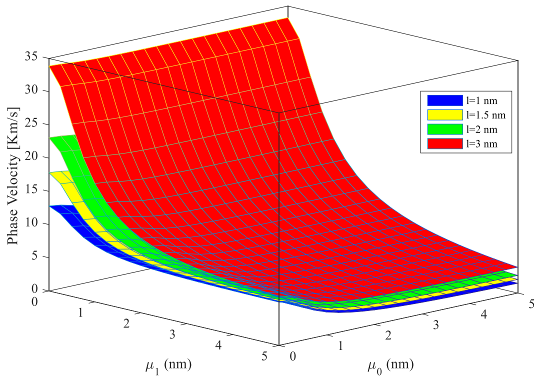

(a)

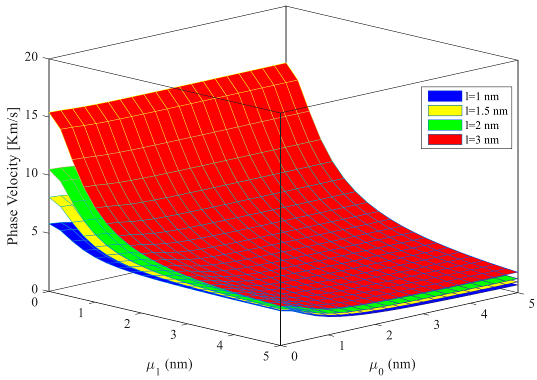

(b)

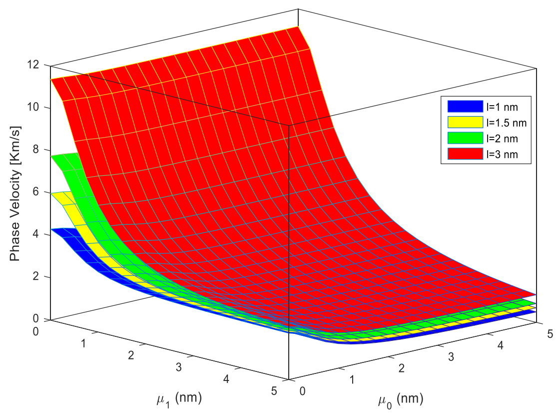

(c)

Fig. 7 Effect of strain gradient length scale parameter on the three pairs of distinct dispersion modes of anisotropic nanoplates with respect to nonlocal parameters (k=1 1/nm)

of distinct dispersion modes. In other words, the decreasing effect of lower order nonlocal parameter on the wave frequency of three pairs of distinct dispersion modes increases when the higher order nonlocal parameter increases. It can be seen from Fig. 6 that in the presence of magnetic field, the change of second and third pairs of distinct dispersion modes under the varying magnetic potential can be ignored.

Effects of rising lower and higher order nonlocal parameters on the variations of three pairs of distinct dispersion modes of rectangular anisotropic nanoplates studied in Fig. 7. Results are plotted for different values of strain gradient parameter when k=1 1/nm. As it is expected, with the increase of nonlocal parameters (μ_0 and μ_1) cause decreasing in the phase velocities of anisotropic nanoplates. Moreover, independent of the amount of increase in the gradient parameter, the higher-order nonlocal parameter plays more important role on the phase velocities of anisotropic nanoplates in comparison with the nonlocal parameter of lower-order.

5. Conclusions

A size-dependent three-dimensional model is reported to study the magnetic field affected wave propagation of rectangular nanoplates made of anisotropic materials for the first time including three small scale parameters. The effects of small scale parameters, wave number, and biaxial magnetic field on the wave characteristics of the nanoplates made are discussed in detail. Small scale parameters have a prominent effect on characteristics of wave propagation. The lower/-higher order nonlocal parameters and strain gradient parameter, respectively, decrease and increases the wave frequency as well as phase velocity. The results obtained by the nonlocal strain gradient theory can be the same or different from those obtained by the classical continuum model depending on the amount of the ratio of the two scale parameters. Further, the wave frequencies are growing with the rising of magnetic potential for some pairs of distinct dispersion modes.

References

Aguiar, A.R., Bravo-Castillero, J. and Da Silva, U.P. (2018), "Application of Mori-Tanaka method in 3-1 porous piezoelectric medium of crystal class 6", *Int. J. Eng. Sci.*, **123**, 36-50.

Alibeigloo, A. and Liew, K. (2014), "Free vibration analysis of sandwich cylindrical panel with functionally graded core using three-dimensional theory of elasticity", *Compos. Struct.*, **113**, 23-30.

Barati, M.R. (2017a), "On wave propagation in nanoporous materials", *Int. J. Eng. Sci.*, **116**, 1-11.

Barati, M.R. (2017b), "Vibration analysis of FG nanoplates with nanovoids on viscoelastic substrate under hygro-thermo-mechanical loading using nonlocal strain gradient theory", *Struct. Eng. Mech.*, **64**(6), 683-693.

Barati, M.R. (2018), "Vibration analysis of porous FG nanoshells with even and uneven porosity distributions using nonlocal strain gradient elasticity", *Acta Mech.*, **229**(3), 1183-1196.

Barretta, R., Faghidian, S.A. and Luciano, R. (2018), "Longitudinal vibrations of nano-rods by stress-driven integral elasticity", *Mech. Adv. Mater. Struct.*, 1-9.

Bellifa, H., Benrahou, K.H., Bousahla, A.A., Tounsi, A. and Mahmoud, S. (2017), "A nonlocal zeroth-order shear deformation theory for nonlinear postbuckling of nanobeams", *Struct. Eng. Mech.*, **62**(6), 695-702.

Besseghier, A., Houari, M.S.A., Tounsi, A. and Mahmoud, S. (2017), "Free vibration analysis of embedded nanosize FG plates using a new nonlocal trigonometric shear deformation theory", *Smart Struct. Syst.*, **19**(6), 601-614.

Besseghier, A., Tounsi, A., Houari, M.S.A., Benzair, A., Boumia, L.

and Heireche, H. (2011), "Thermal effect on wave propagation in double-walled carbon nanotubes embedded in a polymer matrix using nonlocal elasticity", *Phys. E: Low-Dimens. Syst. Nanostruct.*, **43**(7), 1379-1386.

Boumia, L., Zidour, M., Benzair, A. and Tounsi, A. (2014), "A Timoshenko beam model for vibration analysis of chiral single-walled carbon nanotubes", *Phys. E Low-Dimens. Syst. Nanostruct.*, **59**, 186-191.

Bounouara, F., Benrahou, K.H., Belkorissat, I. and Tounsi, A. (2016), "A nonlocal zeroth-order shear deformation theory for free vibration of functionally graded nanoscale plates resting on elastic foundation", *Steel Compos. Struct.*, **20**(2), 227-249.

Brach, S., Dormieux, L., Kondo, D. and Vairo, G. (2017), "Strength properties of nanoporous materials: a 3-layered based non-linear homogenization approach with interface effects", *Int. J. Eng. Sci.*, **115**, 28-42.

Ebrahimi, F. and Barati, M.R. (2018), "Wave propagation analysis of smart strain gradient piezo-magneto-elastic nonlocal beams", *Struct. Eng. Mech.*, **66**(2), 237-248.

Ebrahimi, F. and Dabbagh, A. (2018), "Wave dispersion characteristics of nonlocal strain gradient double-layered graphene sheets in hygro-thermal environments", *Struct. Eng. Mech.*, **65**(6), 645-656.

Ehyaei, J. and Akbarizadeh, M.R. (2017), "Vibration analysis of micro composite thin beam based on modified couple stress", *Struct. Eng. Mech.*, **64**(4), 403-411.

Eringen, A.C. (1983), "On differential equations of nonlocal elasticity and solutions of screw dislocation and surface waves", *J. Appl. Phys.*, **54**(9), 4703-4710.

Eringen, A.C. and Edelen, D. (1972), "On nonlocal elasticity", *Int. J. Eng. Sci.*, **10**(3), 233-248.

Faleh, N.M., Ahmed, R.A. and Fenjan, R.M. (2018), "On vibrations of porous FG nanoshells", *Int. J. Eng. Sci.*, **133**, 1-14.

Ghayesh, M.H. (2018a), "Dynamics of functionally graded viscoelastic microbeams", *Int. J. Eng. Sci.*, **124**, 115-131.

Ghayesh, M.H. (2018b), "Functionally graded microbeams: Simultaneous presence of imperfection and viscoelasticity", *Int. J. Mech. Sci.*, **140**, 339-350.

Ghayesh, M.H. (2018c), "Nonlinear vibration analysis of axially functionally graded shear-deformable tapered beams", *Appl. Math. Modell.*, **59**, 583-596.

Ghayesh, M.H. and Farokhi, H. (2015), "Chaotic motion of a parametrically excited microbeam", *Int. J. Eng. Sci.*, **96**, 34-45.

Gholipour, A., Farokhi, H. and Ghayesh, M.H. (2015), "In-plane and out-of-plane nonlinear size-dependent dynamics of microplates", *Nonlin. Dyn.*, **79**(3), 1771-1785.

Kaghazian, A., Hajnayeb, A. and Foruzande, H. (2017), "Free vibration analysis of a piezoelectric nanobeam using nonlocal elasticity theory", *Struct. Eng. Mech.*, **61**(5), 617-624.

Karami, B. and Janghorban, M. (2016), "Effect of magnetic field on the wave propagation in nanoplates based on strain gradient theory with one parameter and two-variable refined plate theory", *Mod. Phys. Lett. B*, **30**(36), 1650421.

Karami, B., Janghorban, M. and Li, L. (2018a), "On guided wave propagation in fully clamped porous functionally graded nanoplates", *Acta Astronaut.*, **143**, 380-390.

Karami, B., Janghorban, M., Shahsavari, D. and Tounsi, A. (2018b), "A size-dependent quasi-3D model for wave dispersion analysis of FG nanoplates", *Steel Compos. Struct.*, **28**(1), 99-110.

Karami, B., Janghorban, M. and Tounsi, A. (2017), "Effects of triaxial magnetic field on the anisotropic nanoplates", *Steel Compos. Struct.*, **25**(3), 361-374.

Karami, B., Janghorban, M. and Tounsi, A. (2018c), "Galerkin's approach for buckling analysis of functionally graded anisotropic nanoplates/different boundary conditions", *Eng. Comput.*, 1-20.

Karami, B., Janghorban, M. and Tounsi, A. (2018d), "Nonlocal strain gradient 3D elasticity theory for anisotropic spherical nanoparticles", *Steel Compos. Struct.*, **27**(2), 201-216.

Karami, B., Janghorban, M. and Tounsi, A. (2018e), "Variational approach for wave dispersion in anisotropic doubly-curved nanoshells based on a new nonlocal strain gradient higher order shell theory", *Thin-Wall. Struct.*, **129**, 251-264.

Karami, B., Shahsavari, D. and Janghorban, M. (2018f), "A comprehensive analytical study on functionally graded carbon nanotube-reinforced composite plates", *Aerosp. Sci. Technol.*, **82**, 499-512.

Karami, B., Shahsavari, D. and Janghorban, M. (2018g), "Wave propagation analysis in functionally graded (FG) nanoplates under in-plane magnetic field based on nonlocal strain gradient theory and four variable refined plate theory", *Mech. Adv. Mater. Struct.*, **25**(12), 1047-1057.

Karami, B., Shahsavari, D., Janghorban, M., Dimitri, R. and Tornabene, F. (2019a), "Wave propagation of porous nanoshells", *Nanomater.*, **9**(1), 22.

Karami, B., Shahsavari, D., Janghorban, M. and Li, L. (2018h), "Wave dispersion of mounted graphene with initial stress", *Thin-Wall. Struct.*, **122**, 102-111.

Karami, B., Shahsavari, D., Karami, M. and Li, L. (2018i), "Hygrothermal wave characteristic of nanobeam-type inhomogeneous materials with porosity under magnetic field", *Proceedings of the Institution of Mechanical Engineers, Part C: Journal of Mechanical Engineering Science*.

Karami, B., Shahsavari, D. and Li, L. (2018j), "Hygrothermal wave propagation in viscoelastic graphene under in-plane magnetic field based on nonlocal strain gradient theory", *Phys. E: Low-Dimens. Syst. Nanostruct.*, **97**, 317-327.

Karami, B., Shahsavari, D. and Li, L. (2018k), "Temperature-dependent flexural wave propagation in nanoplate-type porous heterogenous material subjected to in-plane magnetic field", *J. Therm. Stress.*, **41**(4), 483-499.

Karami, B., Shahsavari, D., Li, L., Karami, M. and Janghorban, M. (2019b), "Thermal buckling of embedded sandwich piezoelectric nanoplates with functionally graded core by a nonlocal second-order shear deformation theory", *Proceedings of the Institution of Mechanical Engineers, Part C: Journal of Mechanical Engineering Science*, **233**(1), 287-301.

Karami, B., Shahsavari, D., Nazemosadat, S.M.R., Li, L. and Ebrahimi, A. (2018l), "Thermal buckling of smart porous functionally graded nanobeam rested on Kerr foundation", *Steel Compos. Struct.*, **29**(3), 349-362.

Katariya, P.V. and Panda, S.K. (2018), "Frequency and deflection responses of shear deformable skew sandwich curved shell panel: A finite element approach", *Arab. J. Sci. Eng.*, 1-18.

Khaniki, H.B. (2018), "On vibrations of nanobeam systems", *Int. J. Eng. Sci.*, **124**, 85-103.

Khetir, H., Bouiadjra, M.B., Houari, M.S.A., Tounsi, A. and Mahmoud, S. (2017), "A new nonlocal trigonometric shear deformation theory for thermal buckling analysis of embedded nanosize FG plates", *Struct. Eng. Mech.*, **64**(4), 391-402.

Kocaturk, T. and Akbas, S.D. (2013), "Wave propagation in a microbeam based on the modified couple stress theory", *Struct. Eng. Mech.*, **46**(3), 417-431.

Li, L. and Hu, Y. (2015), "Buckling analysis of size-dependent nonlinear beams based on a nonlocal strain gradient theory", *Int. J. Eng. Sci.*, **97**, 84-94.

Li, L. and Hu, Y. (2016), "Wave propagation in fluid-conveying viscoelastic carbon nanotubes based on nonlocal strain gradient theory", *Comput. Mater. Sci.*, **112**, 282-288.

Li, L., Li, X. and Hu, Y. (2016), "Free vibration analysis of nonlocal strain gradient beams made of functionally graded material", *Int. J. Eng. Sci.*, **102**, 77-92.

Li, L., Tang, H. and Hu, Y. (2018), "The effect of thickness on the mechanics of nanobeams", *Int. J. Eng. Sci.*, **123**, 81-91.

Lim, C., Zhang, G. and Reddy, J. (2015), "A higher-order nonlocal elasticity and strain gradient theory and its applications in wave propagation", *J. Mech. Phys. Sol.*, **78**, 298-313.

Malekzadeh, P. (2009), "Three-dimensional free vibration analysis of thick functionally graded plates on elastic foundations", *Compos. Struct.*, **89**(3), 367-373.

Malekzadeh, P. and Heydarpour, Y. (2015), "Mixed Navier-layerwise differential quadrature three-dimensional static and free vibration analysis of functionally graded carbon nanotube reinforced composite laminated plates", *Meccan.*, **50**(1), 143-167.

Mehar, K., Mahapatra, T.R., Panda, S.K., Katariya, P.V. and Tompe, U.K. (2018), "Finite-element solution to nonlocal elasticity and scale effect on frequency behavior of shear deformable nanoplate structure", *J. Eng. Mech.*, **144**(9), 04018094.

Mehar, K. and Panda, S.K. (2018a), *Dynamic esponse of Functionally Graded Carbon Nanotube Reinforced Sandwich Plate*, IOP Conference Series: Materials Science and Engineering, IOP Publishing.

Mehar, K. and Panda, S.K. (2018b), "Theoretical deflection analysis of multi-walled carbon nanotube reinforced sandwich panel and experimental verification", *Compos. Part B: Eng.*

Mehrabian, A. (2018), "The poroelastic constants of multiple-porosity solids", *Int. J. Eng. Sci.*, **132**, 97-104.

Mehralian, F. and Beni, Y.T. (2018), "Vibration analysis of size-dependent bimorph functionally graded piezoelectric cylindrical shell based on nonlocal strain gradient theory", *J. Brazil. Soc. Mech. Sci. Eng.*, **40**(1), 27.

Mehralian, F., Beni, Y.T. and Zeverdejani, M.K. (2017), "Nonlocal strain gradient theory calibration using molecular dynamics simulation based on small scale vibration of nanotubes", *Phys. B: Condens. Matt.*, **514**, 61-69.

Mohammadi, K., Mahinzare, M., Ghorbani, K. and Ghadiri, M. (2018), "Cylindrical functionally graded shell model based on the first order shear deformation nonlocal strain gradient elasticity theory", *Microsyst. Technol.*, **24**(2), 1133-1146.

Mouli, C.B., Ramji, K., Kar, V.R., Panda, S.K., Anil, L.K. and Pandey, H.K. (2018), "Numerical study of temperature dependent eigenfrequency responses of tilted functionally graded shallow shell structures", *Struct. Eng. Mech.*, **68**(5), 527-536.

Murmu, T., McCarthy, M. and Adhikari, S. (2013), "In-plane magnetic field affected transverse vibration of embedded single-layer graphene sheets using equivalent nonlocal elasticity approach", *Compos. Struct.*, **96**, 57-63.

Nami, M.R. and Janghorban, M. (2014a), "Resonance behavior of FG rectangular micro/nano plate based on nonlocal elasticity theory and strain gradient theory with one gradient constant", *Compos. Struct.*, **111**, 349-353.

Nami, M.R. and Janghorban, M. (2014b), "Wave propagation in rectangular nanoplates based on strain gradient theory with one gradient parameter with considering initial stress", *Mod. Phys. Lett. B*, **28**(3), 1450021.

Sahmani, S. and Aghdam, M. (2017a), "Nonlocal strain gradient beam model for nonlinear vibration of prebuckled and postbuckled multilayer functionally graded GPLRC nanobeams", *Compos. Struct.*, **179**, 77-88.

Sahmani, S. and Aghdam, M. (2017b), "A nonlocal strain gradient hyperbolic shear deformable shell model for radial postbuckling analysis of functionally graded multilayer GPLRC nanoshells", *Compos. Struct.*, **178**, 97-109.

Sahmani, S. and Aghdam, M. (2018), "Nonlocal strain gradient beam model for postbuckling and associated vibrational response of lipid supramolecular protein micro/nano-tubules", *Math. Biosci.*, **295**, 24-35.

Sahmani, S., Bahrami, M. and Aghdam, M. (2015), "Surface stress effects on the postbuckling behavior of geometrically imperfect cylindrical nanoshells subjected to combined axial and radial compressions", *Int. J. Mech. Sci.*, **100**, 1-22.

Shafiei, N. and She, G.L. (2018), "On vibration of functionally graded nano-tubes in the thermal environment", *Int. J. Eng. Sci.*, **133**, 84-98.

Shahsavari, D. and Janghorban, M. (2017), "Bending and shearing responses for dynamic analysis of single-layer graphene sheets under moving load", *J. Brazil. Soc. Mech. Sciv Eng.*, **39**(10), 3849-3861.

Shahsavari, D., Karami, B., Fahham, H.R. and Li, L. (2018a), "On the shear buckling of porous nanoplates using a new size-dependent quasi-3D shear deformation theory", *Acta Mech.*, **229**(11), 4549-4573.

Shahsavari, D., Karami, B., Janghorban, M. and Li, L. (2017), "Dynamic characteristics of viscoelastic nanoplates under moving load embedded within visco-Pasternak substrate and hygrothermal environment", *Mater. Res. Expr.*, **4**(8), 085013.

Shahsavari, D., Karami, B. and Li, L. (2018b), "Damped vibration of a graphene sheet using a higher-order nonlocal strain-gradient Kirchhoff plate model", *Compt. Rend. Mécaniq.*, **346**(12), 1216-1232.

Shahsavari, D., Karami, B. and Li, L. (2018c), "A high-order gradient model for wave propagation analysis of porous FG nanoplates", *Steel Compos. Struct.*, **29**(1), 53-66.

Shahsavari, D., Karami, B. and Mansouri, S. (2018d), "Shear buckling of single layer graphene sheets in hygrothermal environment resting on elastic foundation based on different nonlocal strain gradient theories", *Eur. J. Mech.-A/Sol.*, **67**, 200-214.

Shahsavari, D., Shahsavari, M., Li, L. and Karami, B. (2018e), "A novel quasi-3D hyperbolic theory for free vibration of FG plates with porosities resting on Winkler/Pasternak/Kerr foundation", *Aerosp. Sci. Technol.*, **72**, 134-149.

Shahverdi, H. and Barati, M.R. (2017), "Vibration analysis of porous functionally graded nanoplates", *Int. J. Eng. Sci.*, **120**, 82-99.

She, G.L., Ren, Y.R., Yuan, F.G. and Xiao, W.S. (2018a), "On vibrations of porous nanotubes", *Int. J. Eng. Sci.*, **125**, 23-35.

She, G.L., Yan, K.M., Zhang, Y.L., Liu, H.B. and Ren, Y.R. (2018b), "Wave propagation of functionally graded porous nanobeams based on non-local strain gradient theory", *Eur. Phys. J. Plus*, **133**(9), 368.

She, G.L., Yuan, F.G., Karami, B., Ren, Y.R. and Xiao, W.S. (2019), "On nonlinear bending behavior of FG porous curved nanotubes", *Int. J. Eng. Sci.*, **135**, 58-74.

She, G.L., Yuan, F.G. and Ren, Y.R. (2018c), "On wave propagation of porous nanotubes", *Int. J. Eng. Sci.*, **130**, 62-74.

She, G.L., Yuan, F.G., Ren, Y.R., Liu, H.B. and Xiao, W.S. (2018d), "Nonlinear bending and vibration analysis of functionally graded porous tubes via a nonlocal strain gradient theory", *Compos. Struct.*, **203**, 614-623.

She, G.L., Yuan, F.G., Ren, Y.R. and Xiao, W.S. (2017), "On buckling and postbuckling behavior of nanotubes", *Int. J. Eng. Sci.*, **121**, 130-142.

Srinivas, S., Rao, C.J. and Rao, A. (1970), "An exact analysis for vibration of simply-supported homogeneous and laminated thick rectangular plates", *J. Sound Vibr.*, **12**(2), 187-199.

Trofimov, A., Abaimov, S., Akhatov, I. and Sevostianov, I. (2018), "On the bounds of applicability of two-step homogenization technique for porous materials", *Int. J. Eng. Sci.*, **123**, 117-126.

Xu, X.J., Zheng, M.L. and Wang, X.C. (2017), "On vibrations of nonlocal rods: Boundary conditions, exact solutions and their asymptotics", *Int. J. Eng. Sci.*, **119**, 217-231.

Zeighampour, H., Beni, Y.T. and Dehkordi, M.B. (2018), "Wave propagation in viscoelastic thin cylindrical nanoshell resting on a visco-Pasternak foundation based on nonlocal strain gradient

theory", *Thin-Wall. Struct.*, **122**, 378-386.
Zhu, X. and Li, L. (2017), "On longitudinal dynamics of nanorods", *Int. J. Eng. Sci.*, **120**, 129-145.

CC